Supramolecular Chemistry
Publication details, including instructions for authors and subscription information:
http://www.informaworld.com/smpp/title~content=t713649759

Controlling the Amplification of Chirality in Hydrogen-bonded Assemblies

Miguel A. Mateos-Timoneda[a]; Mercedes Crego-Calama[a]; David N. Reinhoudt[a]
[a] Laboratory of Supramolecular Chemistry and Technology, MESA Institute for Nanotechnology and Faculty of Science and Technology, University of Twente, Enschede, The Netherlands

To cite this Article Mateos-Timoneda, Miguel A. , Crego-Calama, Mercedes and Reinhoudt, David N.(2005) 'Controlling the Amplification of Chirality in Hydrogen-bonded Assemblies', Supramolecular Chemistry, 17: 1, 67 — 79
To link to this Article: DOI: 10.1080/10610270412331328826
URL: http://dx.doi.org/10.1080/10610270412331328826

Supramolecular Chemistry, January–March 2005 Vol. 17 (1–2), pp. 67–79

Taylor & Francis
Taylor & Francis Group

Controlling the Amplification of Chirality in Hydrogen-bonded Assemblies

MIGUEL A. MATEOS-TIMONEDA, MERCEDES CREGO-CALAMA* and DAVID N. REINHOUDT

Laboratory of Supramolecular Chemistry and Technology, MESA+ Institute for Nanotechnology and Faculty of Science and Technology, University of Twente, P.O. Box 217, 7500 AE Enschede, The Netherlands

Received (in Austin, USA) 8 July 2004; In final form 9 September 2004

The amplification of chirality (a high enantiomeric or diastereomeric excess induced by a small initial amount of chiral bias) on hydrogen-bonded assemblies has been studied using "sergeants-and-soldiers" experiments under thermodynamically controlled conditions. Here it is shown that different substitutions and structural variations in the building blocks that form these self-assembled systems can be used to control the extent of the chiral amplification.

Keywords: Amplification of chirality; Noncovalent synthesis; Hydrogen bonds; Supramolecular chemistry

INTRODUCTION

Amplification of chirality is the process from which a high enantiomeric or diastereomeric excess (*e.e.* or *d.e.*, respectively) is induced by a small initial amount of chiral bias [1]. Chiral amplification is a widely study process due to its implications for the origin of life and in enantioselective autocatalytic processes [1–5]. Green *et al.* first reported the amplification of chirality in polyisocyanate polymers possessing a stiff helical backbone. The helicity of this backbone can be controlled via the insertion of chiral centers in the peripheral groups. The optical activity of the polymer remains constant even when the percentage of chiral units is lowered to 5%. This phenomenon is referred as the "sergeants-and-soldiers" principle [6]: the achiral units are forced to follow the helicity induced by the chiral units. This phenomenon has been widely studied in covalent and noncovalent polymers [7–14]. A good example has been reported by Masuda *et al.*, who used "sergeants-and-soldiers" experiments to study the assembly of helical columns of supramolecular hydrogen-bonded polymers [15]. Additionally, several theoretical models have been developed to fit the *amplified* experimental data and to obtain the parameters that govern the amplification of chirality in polymeric structures [16–20]. Recently, chiral amplification has also been studied in the formation of solid polymer films [21], in the recognition of chiral amines and amino alcohols by optically inactive polyacetylenes [22,23] and other supramolecular assemblies [24,25], in the cyclodimerization of saddle-shape porphyrins upon interaction with mandelic acid [26], and in the formation of chiral liquid crystalline phases [27–30].

Previously, our group showed, for the first time, that the "sergeants-and-soldiers" principle also applies to dynamic hydrogen-bonded assemblies of well-defined (finite) molecular composition [31]. It was shown that the dissociation rate of the dimelamine components influences the thermodynamics of chiral amplification; that is a decrease in the dissociation rate constant causes a larger amplification of chirality. Furthermore, model simulations showed that it would be possible to achieve high chiral amplification ($d.e. > 99\%$) in these dynamic systems even when only 0.1% of the components is chiral. Here, we describe a more extensive study on the amplification of chirality in double-rosette hydrogen-bonded assemblies under thermodynamically controlled conditions. A large variety of systems comprising chiral and racemic structurally closely related assemblies $\mathbf{1}_3{\cdot}(CYA)_6$ are studied in order to determine which parameters govern the extent of amplification of chirality for these

*Corresponding author: m.cregocalama@utwente.nl

ISSN 1061-0278 print/ISSN 1029-0478 online © 2005 Taylor & Francis Ltd
DOI: 10.1080/10610270412331328826

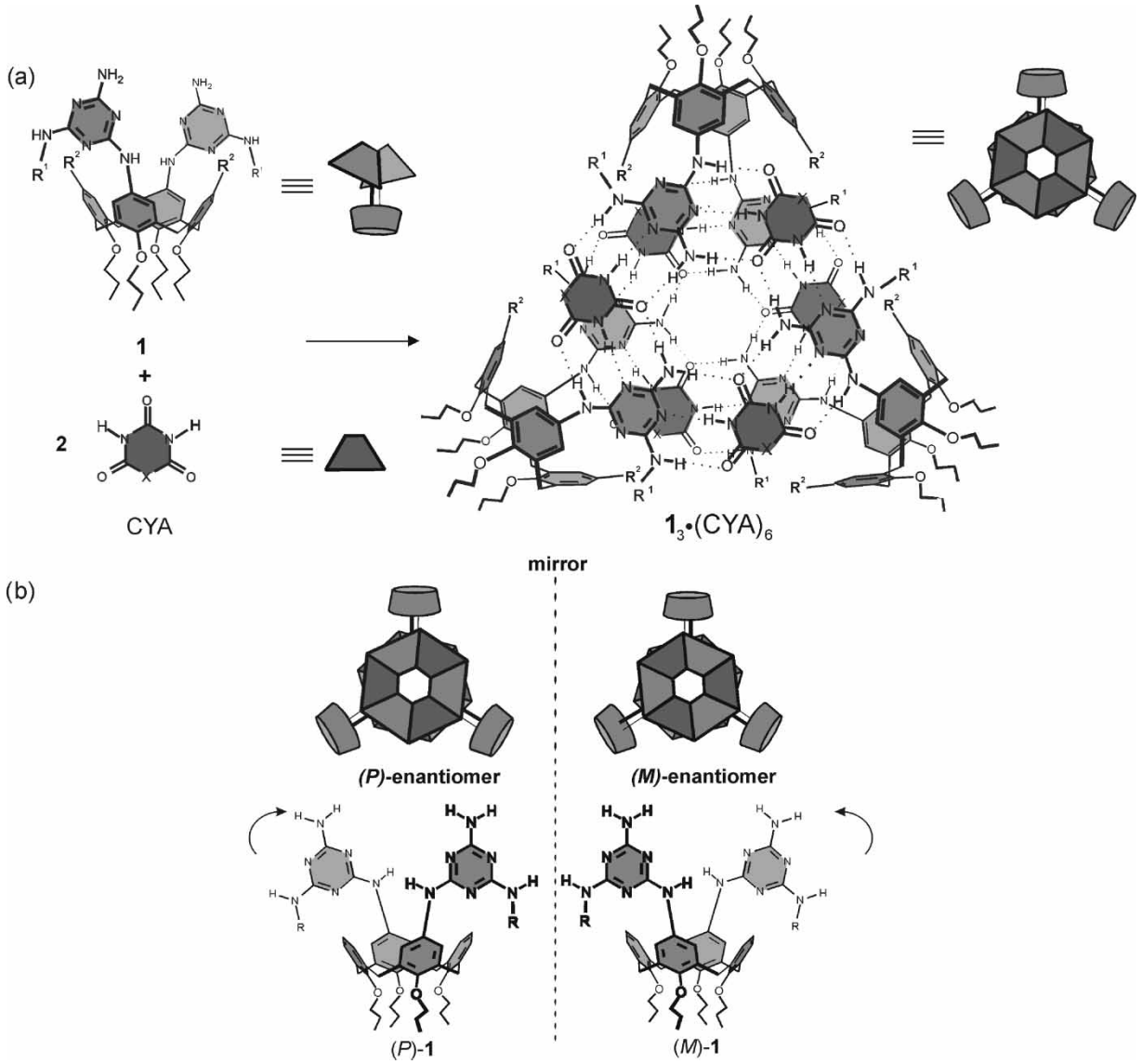

FIGURE 1 Schematic representation of (a) the molecular building blocks and their self-assembly into double rosettes $\mathbf{1}_3$·(CYA)$_6$ and (b) the (*P*)- and (*M*)-enantiomers and the orientation of their two melamine fragments.

types of hydrogen-bonded assemblies. Structural variations within the building blocks have been introduced in three different positions, that is in the two melamine moieties and the calix[4]arene skeleton (**1**), and the chiral cyanurate (*CYA) (see Fig. 1).

RESULTS AND DISCUSSION

Earlier studies have shown that hydrogen-bonded double-rosette assemblies $\mathbf{1}_3$·(CYA/*CYA)$_6$ are formed spontaneously by mixing calix[4]arene dimelamines **1** with 2 equivalents of cyanurates (CYA = achiral and *CYA = chiral) in apolar solvents, such as chloroform, benzene and toluene (Fig. 1) [32,33]. The assembly formation is driven by the formation of 36 complementary hydrogen bonds between the donor–acceptor–donor (DAD) array of the calix[4]arene dimelamine and acceptor–donor–acceptor (ADA) array of the cyanurate building blocks. These assemblies can exist in three different isomeric forms with D_3, C_{3h} and C_s symmetry [34]. The assemblies with D_3 symmetry, which is the predominant isomer, are chiral due to the staggered orientation of the two melamine fragments, leading to a twist of the two different rosette planes, which can adopt either a clockwise [(*P*)-isomer] or a counterclockwise [(*M*)-isomer] conformation (Fig. 1). In the absence of any center of chirality, the assemblies are formed as a racemic mixture of both (*P*)- and (*M*)-enantiomers. However, upon introduction of chiral centers in one of the molecular components of the assembly (calix[4]arene dimelamines or cyanurates), only one of the two possible diastereoisomers is formed with a *d.e.* up to 96% [35,36]. When chiral cyanurates are used, the sense of the twist of the melamine

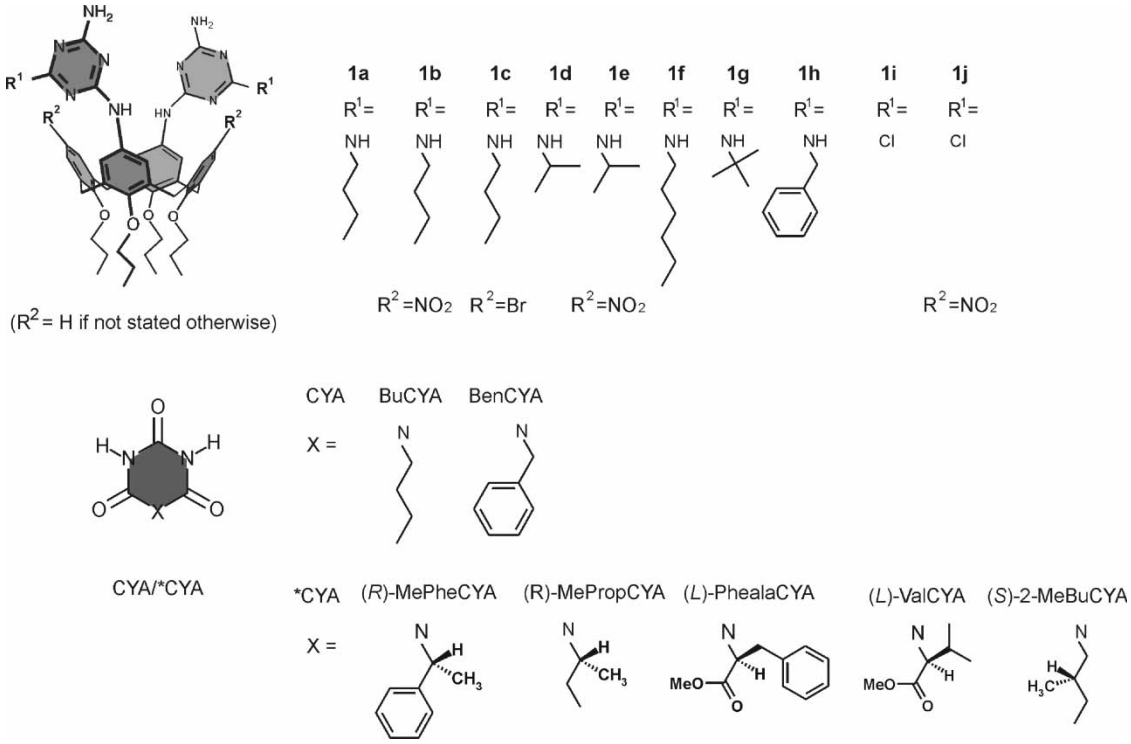

fragments is dictated by the stereochemistry of the chiral center in the cyanurates, that is a cyanurate bearing a chiral center with (*R*)-stereochemistry leads only to the formation of, for example, the (*P*)-diastereomer, while the (*S*)-isomer then leads only to the (*M*)-diastereomer. These chiral (*P*)- and (*M*)-assemblies are highly circular-dichroism (CD) active due to the dissymmetric arrangement of the different chromophores within the rigid structure.

Synthesis

Calix[4]arene dimelamines **1a**–**c**, **1h** and bis(chlorotriazine) calix[4]arene derivatives **1i**–**j** (Chart 1) were synthesizing following literature procedures [33]. Calix[4]arene dimelamines **1d**–**g** were synthesized by reaction of the corresponding bis(chlorotriazine) calix[4]arene **1i**–**j** with an excess of the corresponding amine, that is *i*-propylamine (**1d**,**e**), hexylamine (**1f**) or *t*-butylamine (**1g**), in THF. Cyanurates BuCYA, BenCYA, (*R*)-MePheCYA, (*L*)-PhealaCYA and (*L*)-ValCYA were prepared following literature procedures [36]. Cyanurates (*R*)-MePropCYA and (*S*)-2-MeBuCYA were synthesized in one step via ring closure of the corresponding amine with *N*-chlorocarbonylisocyanate in THF under extremely dry conditions (see experimental section).

Amplification of Chirality in Assemblies $\mathbf{1_3}$·(CYA/*CYA)$_6$

Solutions of the assembly (*P*)-$\mathbf{1b_3}$·((*R*)-MePheCYA)$_6$ and racemic $\mathbf{1b_3}$·(BenCYA)$_6$ in benzene (1 mM) were mixed in ratios ranging from 90:10 to 10:90 and the CD-intensity at 308 nm was measured as a function of time at 70°C. The thermodynamic equilibrium is reached almost immediately after the mixing process (especially for the higher ratios of chiral assembly). From these measurements, the relative CD-intensities were related to a calculated 100% value based on the ratio (*P*)-$\mathbf{1b_3}$·((*R*)-MePheCYA)$_6$/(*P*)-$\mathbf{1b_3}$·(BenCYA)$_6$ and plotted as a function of time (Fig. 2a).[†] It was assumed that all the assemblies present in solution after the mixing process have the same $\Delta\varepsilon_\lambda$ (CD-intensity at the wavelength of maximum absorbance), which seems reasonable regarding their very similar molecular structures and the number of chromophores.[‡] For the high ratio values of (*P*)-$\mathbf{1b_3}$·((*R*)-MePheCYA)$_6$, the CD-intensities at $t = 0$ do not correspond to the initial molar fraction of (*P*)-$\mathbf{1b_3}$·((*R*)-MePheCYA)$_6$, because immediately after mixing the thermodynamic value for $\Delta\varepsilon_\lambda$ is reached (Fig. 2a). In the rest of the text, these thermodynamic values are referred to as relative $\Delta\varepsilon_{\text{therm}}$. If there were no amplification of the chirality in the system, the CD-intensity of the mixtures would increase linearly with

[†]Assembly (*P*)-$\mathbf{1b_3}$·(BenCYA)$_6$, which is formed using an enantioselective process (substitution of a chiral barbiturate derivative for the nonchiral BenCYA) [37], has a slightly lower $\Delta\epsilon$ than assembly (*P*)-$\mathbf{1b_3}$·((*R*)-MePheCYA)$_6$. For this reason, the relative CD intensities were related to the ratio (*P*)-$\mathbf{1b_3}$·((*R*)-MePheCYA)/(*P*)-$\mathbf{1b_3}$·(BenCYA)$_6$.

[‡]Previous studies have shown that assemblies containing similar chromophores exhibit similar CD intensities [31].

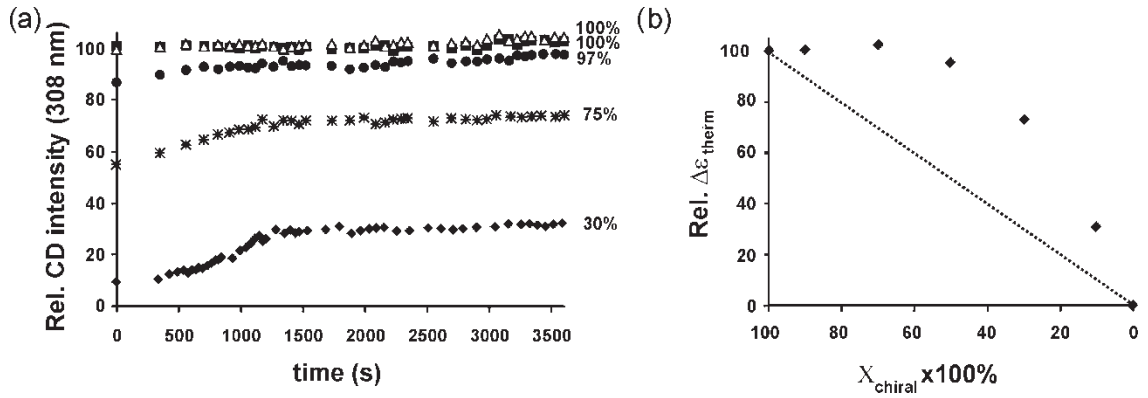

FIGURE 2 (a) Plots of relative CD-intensity at 308 nm versus time for mixtures of (*P*)-**1b**$_3$·((*R*)-MePheCYA)$_6$ and **1b**$_3$·(BenCYA)$_6$ with different initial mole fractions of **1b**$_3$·((*R*)-MePheCYA)$_6$ (◆, 10%; *, 30%; •, 50%; ■, 70%; Δ, 90%) (the percentage values in the graphs represent the relative CD-intensities reached at thermodynamic equilibrium). (b) Plot of relative CD-intensities at thermodynamic equilibrium for different molar fractions of the chiral component. The dotted line represents the expected CD-intensity when there is no amplification of chirality.

the molar fraction of the chiral assembly present; thus a mixture with 50% of chiral assembly will display a CD-intensity corresponding to this 50% of chiral assembly component. However, a plot of the relative $\Delta\varepsilon_{\text{therm}}$ values as a function of the ratio chiral:nonchiral rosette assemblies shows the typical nonlinear behavior of the "sergeants-and-soldiers" principle (Fig. 2b); the CD-intensities of the mixtures increase nonlinearly with the percentage of chiral assembly present [31]. For example, when a 70:30 mixture of **1b**$_3$·(BenCYA)$_6$ and (*P*)-**1b**$_3$·((*R*)-MePheCYA)$_6$ reaches thermodynamic equilibrium, the relative CD-intensity has increased from 30% (expected in the case where there is no chiral amplification) to 75%.

The nonlinear increase in the CD-intensity is due to the exchange between the chiral and nonchiral cyanurates within the assemblies, that is to the presence of the heteromeric assemblies **1b**$_3$·(BenCYA)$_n$((*R*)-MePheCYA)$_{6-n}$ ($n = 1-5$) (Fig. 3). The ^{1}H NMR spectra clearly show the presence of numerous signals in the region of 15 − 14 ppm due to the formation of these heteromeric assemblies (Fig. 3).[¶] The presence of one to five chiral centers ((*R*)-MePhe) in these assemblies leads to the preferential formation of the (*P*)-diastereomer. Thus, these assemblies exhibit a higher *d.e.* than the expected statistical 16% per chiral center in the absence of chiral amplification. This increase in the *d.e.* of the heteromeric assemblies is related to the introduction of a difference in the free energy between the (*P*)- and (*M*)-diastereomers by the chiral centers. Even assembly **1b**$_3$·(BenCYA)$_6$, which does not contain any chiral center, exists in the mixture mainly as the (*P*)-enantiomer due to the exchange process between BenCYA and (*R*)-MePheCYA and the chiral memory effect [37,38].

The curve of amplification of chirality (Fig. 2b) was fitted to a thermodynamic model based on the difference in free energy between the (*P*)- and (*M*)-diastereomers of the homo/heteromeric assemblies **1**$_3$·(CYA)$_n$(*CYA)$_{6-n}$ ($n = 0-6$) at thermodynamic equilibrium. All the equilibria accounted for in the model are depicted in Fig. 4. The formation of the rosette is considered to take place in one step from the different building blocks. The influence of the dissociation rate constant is not included in the model, however, from previous studies it is well known to affect the extent of chiral amplification [31]. Cooperativity is also not included in the model, and therefore ΔG° is assumed to increase linearly with the number of chiral components present. Each chiral substituent present in the unfavorable (*M*)-diastereomer[§] induces a free energy difference $\Delta G^\circ_{M/P}$, which results in a decrease in the equilibrium constant (*K*) between the (*M*)-isomer and the free components with a factor of $f_{\text{m}} = \exp(-\Delta G^\circ_{M/P}/RT)$. For example, for an assembly containing three chiral centers, the equilibrium constant is decreased by a factor of f_{m}^3. The equilibrium constant is assumed to be the same for every assembly. Statistical factors are included in the model accounting for the statistically different possibilities of formation of each assembly. The model only takes the cyanurate components

[¶]The presence of two signals in the region 15 − 14 ppm, where the hydrogen-bonded imide NH protons of the cyanurate components appear, in the ^{1}H NMR spectrum is characteristic for the formation of homomeric hydrogen-bonded double-rosette assemblies **1**$_3$·(CYA/*CYA)$_6$. When heteromeric assemblies are formed, the NH protons are not magnetically equivalent, consequently giving rise to a far more complicated ^{1}H NMR spectrum.

[§]When the chiral centers are in the cyanurate building blocks, a center with (*R*)-stereochemistry generally induced the formation of assemblies with (*P*)-helicity. Thus, when (*R*)-MePheCYA is present the formation of the (*M*)-diastereomer is unfavorable. The cyanurates formed with amino acids residues comprise a special case. All the (*L*)-amino acid base cyanurates [(*S*)-stereochemistry] induce (*P*)-helicity in the corresponding assemblies.

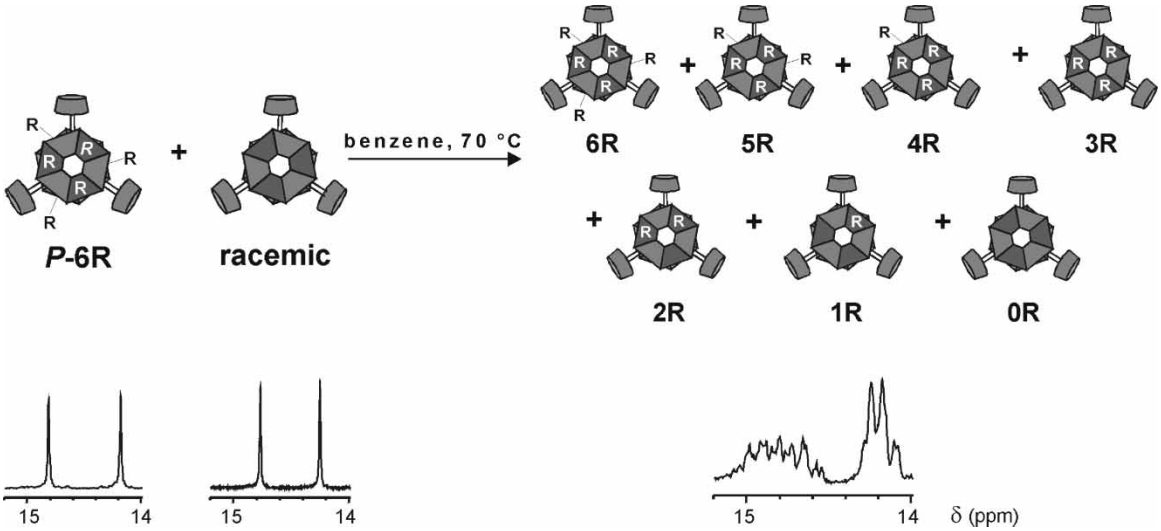

FIGURE 3 Schematic representation of the mixing process and formation of the heteromeric assemblies $\mathbf{1b}_3$·(BenCYA)$_n$((*R*)-MePheCYA)$_{6-n}$ ($n = 1–5$) from the homomeric assemblies $\mathbf{1b}_3$·((*R*)-MePheCYA)$_6$ (*P*-**6R**, where R denotes the chiral group (*R*)-MePhe) and $\mathbf{1b}_3$·(BenCYA)$_6$ (**racemic**) (top) and part of their ^{1}H NMR spectra (bottom). The ^{1}H NMR spectrum of the mixture corresponds to a 1:1 mixture of $\mathbf{1b}_3$·((*R*)-MePheCYA)$_6$ and $\mathbf{1b}_3$·(BenCYA)$_6$ recorded 30 min after mixing. All spectra were recorded in benzene-d_6 at room temperature.

into account and not the calix[4]arene dimelamine moieties because the chirality in the assemblies is introduced by the chiral centers on the cyanurates. Thus, the least-squares fit of the CD-data for the system formed from $\mathbf{1b}_3$·(BenCYA)$_6$ and (*P*)-$\mathbf{1b}_3$·((*R*)-MePheCYA)$_6$ (Fig. 2b) using the model resulted in $\Delta G_{M/P}$ (343 K) = 4.2 kJ mol^{-1} per chiral substituent. This corresponds to a total free energy difference $\Delta G°_{\text{tot}}$ (343 K) = 25.2 kJ mol^{-1} between the favored (*P*)- and the unfavored (*M*)-diastereomers of assembly $\mathbf{1b}_3$·((*R*)-MePheCYA)$_6$ containing six chiral centers.

Influence of the Calix[4]arene Dimelamine Substituents (R^1 and R^2) on the Amplification of Chirality

The extent of the chiral amplification using the thermodynamic model mentioned above was studied for a variety of systems in which the substituent R^1 (Fig. 1) of the dimelamine became gradually bulkier. The influence of the substituent was studied using the systems comprising the dimelamines **1a**, **1d**, **1f**, **1g** and **1h**, bearing butyl-, *i*-propyl-, hexyl-, *t*-butyl- and benzyl-amino functionalities, respectively. (*R*)-MePheCYA was chosen as the chiral cyanurate and BenCYA as the nonchiral cyanurate because both have the same chromophore (phenyl groups) ensuring the same maximum $\Delta\varepsilon_\lambda$ in all the assemblies.

Mixtures of assemblies (*P*)-$\mathbf{1x}_3$·((*R*)-MePheCYA)$_6$ and $\mathbf{1x}_3$·(BenCYA)$_6$ (**x** = **a**, **d**, **f**–**h**) in ratios varying between 90:10 and 10:90 were prepared and the CD-intensity at 300 nm was measured as a function of time at 70°C in benzene. After 30 min the $\Delta\varepsilon_{\text{therm}}$ was reached, and it was plotted versus the molar ratio of chiral assembly. In all the cases, the CD-intensities are significantly higher than the sum of the CD-intensities of the individual assemblies ("sergeants-and-soldiers" behavior). The results for these systems are summarized in Fig. 5 and Table I.

Fitting the experimental data to the thermodynamic model gave the ΔG between the different diastereomers of the assemblies. Analysis of the data shows that increasing the size of the substituents of the melamine moieties results in a decrease in the difference in free energy between the (*P*)- and (*M*)-diastereomers ($\Delta G_{M/P}$). Thus for a 70:30 achiral: chiral assembly for the system formed with calix[4]dimelamine **1a** (R^1 = butyl), the thermodynamic relative CD-intensity increases to 65% (from the expected 30% without amplification), while for the system formed with calix[4]arene dimelamine **1h** (R^1 = benzyl), the thermodynamic value only increases to 44%. These values are related to a difference in the $\Delta G_{M/P}$, decreasing from 3.5 to 1.3 kJ mol^{-1} per chiral center for the systems bearing butyl and benzyl substituents in the calix[4]arene dimelamine ring, respectively, which correspond to a ΔG_{tot} of 21.0 and 7.8 kJ mol^{-1}, respectively, for assemblies (*P*)-$\mathbf{1a}_3$·((*R*)-MePheCYA)$_6$ and (*P*)-$\mathbf{1h}_3$·((*R*)-MePheCYA)$_6$, each containing six chiral substituents.

Upon introduction of bulky substituents on the calix[4]arene dimelamine building block, an increase in $\Delta G_{M/P}$, and therefore an enhanced amplification of chirality (smaller ratio of chiral assembly needed to obtain 100% of relative CD-intensity in achiral: chiral assemblies), was expected. The observed decrease in the $\Delta G_{M/P}$ when bulky substituents are present in the assembly might come from a decrease

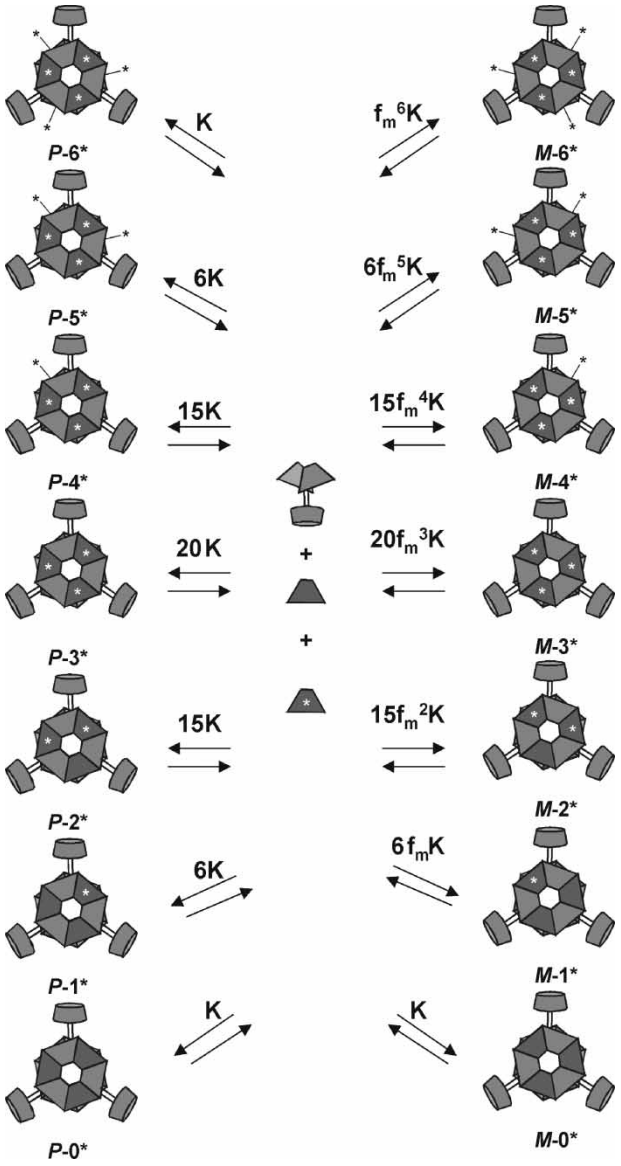

FIGURE 4 Thermodynamic model. Each chiral substituent in assemblies $\mathbf{1}_3$·(CYA)$_n$(*CYA)$_{6-n}$ ($n = 0$–6) lowers the equilibrium constant of the unfavored (*M*)-isomer by a factor $f_m = \exp(-\Delta G^\circ_{M/P}/RT)$ (*denotes the chiral components of the assembly).

of the thermodynamic stability of the system.[‖] To prove this hypothesis, ^{1}H NMR studies of the mixtures after the amplification experiments were performed. Study of the systems (*P*)-$\mathbf{1f}_3$·((*R*)-MePheCYA)$_6$/$\mathbf{1f}_3$·(BenCYA)$_6$ (**1f** = hexyl substituents) and (*P*)-$\mathbf{1g}_3$·((*R*)-MePheCYA)$_6$/$\mathbf{1g}_3$·(BenCYA)$_6$ (**1g** = *t*-butyl substituents) showed that after mixing, the rosettes in the mixture are not formed in 100% yield, as can be deduced by integration of the CH_2-bridged proton resonances of the calix moiety and the hydrogen-bonded NH-proton resonances of the cyanurates. One possible explanation for the thermodynamic destabilization can be extracted from molecular modeling studies (Quanta 97, CHARMm 24.0). The introduction of steric hindrance in the dimelamine moiety induces a twist in the two melamine fragments, and therefore a decrease in the planarity of the rosette floors. This will result in a weaker hydrogen-bond array and a decrease in the stability of the assemblies (Fig. 6).

The effect on the amplification of chirality upon the introduction of substituents in the calix[4]arene skeleton (R^2, Fig. 1) was also studied. For this purpose, calix[4]arene dimelamines substituted with butyl groups in the melamine rings and different substitutions (R^2) [hydrogen (**1a**), nitro (**1b**) and bromide (**1c**) groups] in the calix[4]arene skeleton were synthesized. Mixtures of assemblies (*P*)-$\mathbf{1x}_3$·((*R*)-MePheCYA)$_6$ and $\mathbf{1x}_3$·(BenCYA)$_6$ (**x** = **a**–**c**) in ratios varying between 90:10 and 10:90 (nonchiral:chiral rosette assemblies) were prepared and the CD-intensity at 308 nm was measured as a function of time at 70°C in benzene. The $\Delta\varepsilon_{therm}$ reached after 30 min was plotted versus the molar ratio of the chiral component (Fig. 7). For these systems the CD-intensities also deviate from linearity, showing typical "sergeants-and-soldiers" behavior (Fig. 7).

The data (Fig. 7 and Table II) clearly show that the introduction of groups in the calix[4]arene skeleton has a great influence on the amplification of chirality for these systems. The presence of the nitro substituents (R^2) on the calix[4]arene skeleton (**1b**) increases the value of $\Delta G_{M/P}$ compared with the one lacking substituents in this position (4.2 and 3.5 kJ mol^{-1}, respectively), while the presence of the bromide substituents induces a decrease in $\Delta G_{M/P}$ to 2.0 kJ mol^{-1}. The cause of these large differences is not clear but the large influence exerted by these functional groups could be due to steric (bulkiness of the groups) and/or electronic factors (electrostratic repulsion/attraction) introduced by the substituents in the calix[4]arene skeleton. These factors could influence the conformation of the calix[4]arene skeleton and the strength of the hydrogen bonds and, consequently, the planarity and stability of the rosettes. The introduction of the nitro substituents in the calix[4]arene skeleton (**1b**) slows down the kinetics of the process compared to the introduction of the bromo substituents (**1c**).[#] This is reflected in the time before the amplification of chirality begins.

The presence of nitro groups in the calix[4]arene skeleton has a large effect on the extent of

[‖]We have also studied the thermodynamic stability of $\mathbf{1a}_3$·((*R*)-MePheCYA)$_6$ and $\mathbf{1e}_3$·((*R*)-MePheCYA)$_6$ in polar solvents. The χ value (χ = percentage of polar solvent at which 50% of the assembly is still intact) in MeOH for assemblies $\mathbf{1a}_3$·((*R*)-MePheCYA)$_6$ (butyl chain) and $\mathbf{1e}_3$·((*R*)-MePheCYA)$_6$ (*t*-butyl chain) shows a decrease from 60% to 7.5%, suggesting a decrease in thermodynamic stability of the assemblies upon increasing the bulkiness of the substituents.

[#]The kinetics of the system formed with dimelamine **1b** are slower than the kinetics of the systems formed with **1c** as can be judge by comparing Figs. 5 and 7, respectively. However, it is not possible to determine the kinetic parameters of both chiral amplification processes.

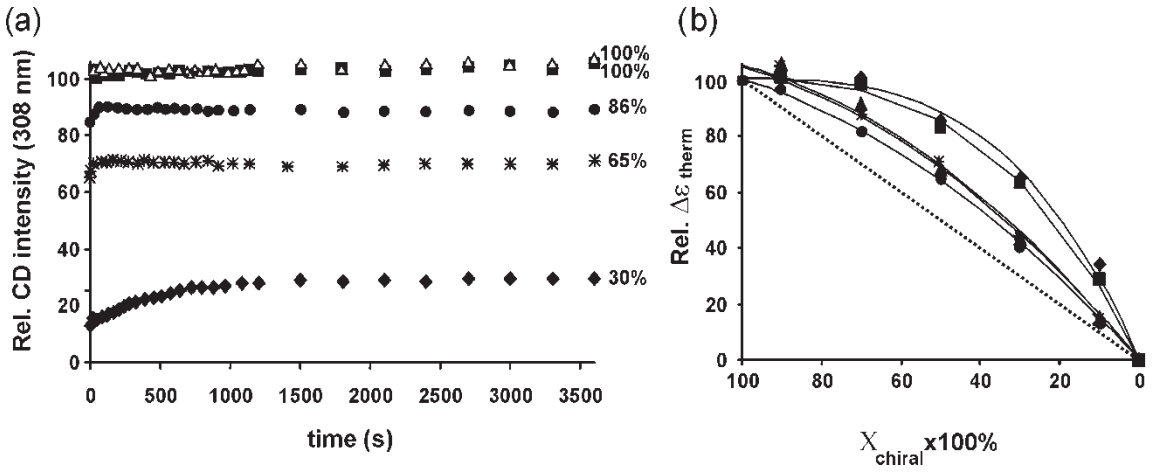

FIGURE 5 (a) Plots of relative CD-intensity measured at 300 nm versus time for mixtures of (*P*)-**1a**$_3$·((*R*)-MePheCYA)$_6$ and **1a**$_3$·(BenCYA)$_6$ with different initial mole fractions of (*P*)-**1a**$_3$·((*R*)-MePheCYA)$_6$ (◆, 10%; *, 30%; •, 50%; ■, 70%; Δ, 90%) (the percentage values in the graphs represent the relative CD-intensities reached at thermodynamic equilibrium). (b) Plot of relative CD-intensities at thermodynamic equilibrium for different mole ratios of the chiral components for different systems (◆, **1a**, ■; **1d**, *; **1f**; ▲, **1g**; •, **1h**). The solid lines represent the calculated best fit using the thermodynamic model. The dotted line represents the expected CD-intensity in the absence of amplification of chirality.

TABLE I Difference in free energy between the (*P*)- and (*M*)-diastereomers of assemblies **1x**$_3$·((*R*)-MePheCYA)$_6$ as a result of the presence of chiral centers in the assembly calculated using the thermodynamic model[a]

1x	$\Delta G_{M/P}$ (kJ mol^{-1})[b]	ΔG_{tot} (kJ mol^{-1})[c]
1a	3.5	21.0
1d	3.0	18.0
1f	1.4	8.4
1g	1.4	8.4
1h	1.3	7.8

[a] [(*P*)-**1x**$_3$·((*R*)-MePheCYA)$_6$] = [**1x**$_3$·(BenCYA)$_6$] = 1.0 mM, 343 K, benzene. [b] Difference in free energy per chiral center. [c] Total free energy difference between (*P*)- and (*M*)-diastereomers of assemblies **1x**$_3$·((*R*)-MePheCYA)$_6$.

amplification of chirality in these dynamic assemblies, leading to systems displaying a large amplification of chirality. For this reason, the influence of the substituent in the dimelamine moiety (R^1) was investigated when the nitro group was present in the calix[4]arene skeleton (R^2). For this purpose, the assemblies formed with the dimelamines **1b** and **1e**, bearing butyl and *i*-propyl substituents, respectively, and nitro substituents in the calix[4]arene skeleton, and the cyanurates (*R*)-MePheCYA and BenCYA were studied. The results obtained are displayed in Table III.

Surprisingly, the presence of sterically demanding substituents in the dimelamine rings of **1e** (*i*-propyl groups) does not influence the degree of amplification of the system when the nitro substituents are present in the calix[4]arene skeleton. The $\Delta G_{M/P}$ for **1e** only decreases by 0.1 kJ mol^{-1} when compared with the melamine **1b** (butyl groups). When the substituents are hydrogens instead of nitro groups the introduction of *i*-propyl groups (**1d**) induces a decrease in the $\Delta G = 0.5$ kJ mol^{-1} when compared with calix[4]arene dimelamines containing butyl groups (**1a**). As explained earlier, the presence of the nitro groups in the calix[4]arene skeleton slows down the exchange of the dimelamine moieties (see Fig. 7a). As shown before [31], this decrease in the dissociation rate constant results in an increase in the chiral amplification.

INFLUENCE OF THE CYANURATE SUBSTITUENT (*X*) ON THE AMPLIFICATION OF CHIRALITY

The amplification of chirality was also studied for systems with different chiral cyanurates [*CYA = (*R*)-MePropCYA, (*R*)-MePheCYA, (*L*)-PhealaCYA and (*L*)-ValCYA], in which the N-substituent gradually increases in size. All these cyanurates have the chiral center in the α-position relative to the nitrogen. The amplification of chirality with (*S*)-2-MeBuCYA with the chiral center in the β-position was also studied.

Mixtures of assemblies (*P*)-**1a**$_3$·(*CYA)$_6$ and **1a**$_3$·(CYA)$_6$ [*CYA = (*R*)-MePropCYA,[**] (*R*)-MePheCYA, (*L*)-PhealaCYA and (*L*)-ValCYA; CYA = BenCYA and BuCYA] in ratios varying between 90:10 and 10:90 were prepared and the CD-intensity at 300 nm was measured as a function of time at 70°C in benzene. Immediately the $\Delta\varepsilon_{therm}$ was reached, and it was plotted versus the molar ratio of chiral assembly (Table IV and Fig. 8).

As can be deduced from the data and contrary to what happens with the substitution in

[**]For the system formed with (*R*)-MePropCYA and (*L*)-ValCYA, the achiral cyanurate BuCYA was chosen.

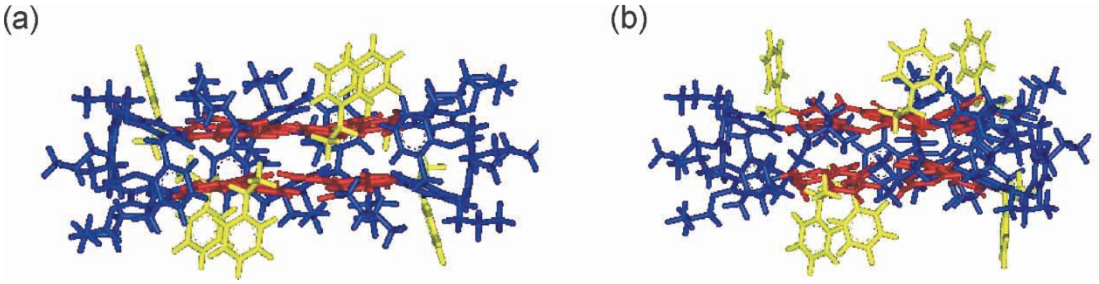

FIGURE 6 Gas-phase minimized structures of assemblies (a) $\mathbf{1a}_3$·(*R*)-MePheCYA$_6$ and (b) $\mathbf{1g}_3$·(*R*)-MePheCYA$_6$ bearing butyl and *t*-butyl chains in the dimelamine moiety, respectively. The calix[4]arene moieties are depicted in blue, the rosette motifs in red and the (*R*)-MePhe chiral groups of the cyanurate compounds in yellow.

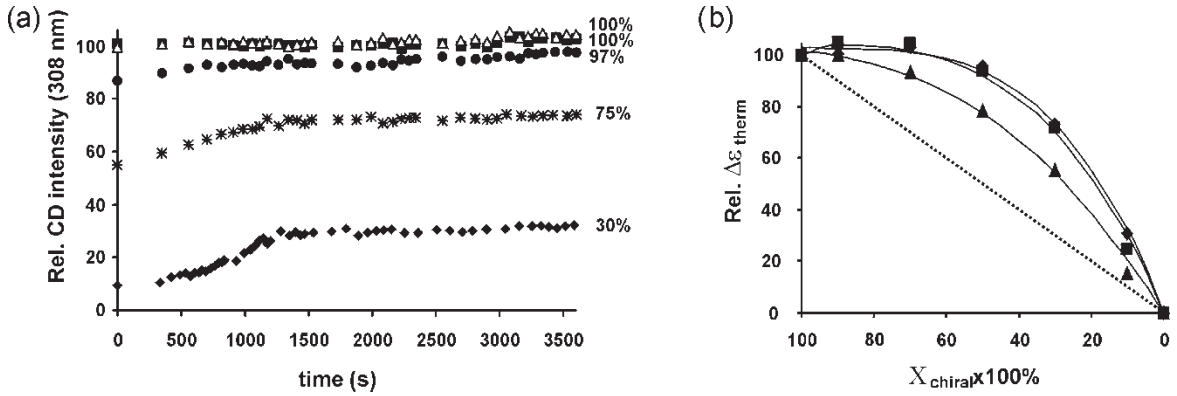

FIGURE 7 (a) Plots of relative CD intensity (at 308 nm) against time for mixtures of (*P*)-$\mathbf{1b}_3$·((*R*)-MePheCYA)$_6$ and $\mathbf{1b}_3$·(BenCYA)$_6$ with different initial mole fractions of $\mathbf{1b}_3$·((*R*)-MePheCYA)$_6$ (◆, 10%; *, 30%; •, 50%; ■, 70%; Δ, 90%) (the percentage values in the graphs represent the relative CD-intensities reached at thermodynamic equilibrium). (b) Plot of relative CD-intensities at thermodynamic equilibrium for different mole ratios of the chiral component (■, **1a**: ◆, **1b**; ▲, **1c**). The solid lines represent the calculated best fit using the thermodynamic model described previously. The dotted line represents the expected CD-intensity in the absence of amplification of chirality.

the calix[4]arene dimelamine building blocks, the introduction of substituents in the cyanurate component that are less sterically demanding decreases the difference in free energy between the (*P*)- and (*M*)-diastereomers. For example, the difference in the free energy introduced by one chiral center for (*R*)-MePheCYA is 3.5 kJ mol^{-1}, while this difference drops to 1.9 kJ mol^{-1} with the less bulky cyanurate (*R*)-MePropCYA. The introduction of bulky amino acids as chiral residues in cyanurates (*L*)-PhealaCYA and (*L*)-ValCYA also decreases the degree of the chiral amplification. For all these systems, the decrease in the chiral amplification might come from the decrease in the rigidity of the assemblies.

The amplification of chirality in systems in which the chirality center is further away from the core of the assembly was also studied. For that purpose, the cyanurate (*S*)-2-MeBuCYA, in which the chiral center is in the β-position with respect to the nitrogen atom, was synthesized. However, the ^{1}H NMR spectrum of the assembly $\mathbf{1a}_3$·((*S*)-2-MeBuCYA)$_6$ (Fig. 9) exhibits two sets of two sharp signals with different intensities in the region where the hydrogen-bonded NH-protons of the cyanurate are expected ($\delta = 15$–13 ppm). The unequal intensity of the signals rules out the possible presence of a isomer with C_{3h} symmetry.[††] Therefore, these signals can only be explained by the presence of both (*M*)- and (*P*)-diastereomers. Consequently, the system formed with this cyanurate is not suitable for carrying out the experiments of amplification of chirality because of the lack of total diastereomeric induction.

CONCLUSIONS

The experiments and the thermodynamic model presented here provide a new insight into the amplification of chirality in hydrogen-bonded

[††]Based on symmetry arguments, the isomer with D_3 symmetry bearing chiral centers should have two signals in the ^{1}H NMR spectrum because the two different protons involved in the hydrogen-bonding network reside in a chemically different environment within the assembly. On the other hand, the isomer with C_{3h} symmetry should have four signals of equal intensity in the ^{1}H NMR spectrum.

TABLE II Difference in free energy calculated using the thermodynamic model between the (*P*)- and (*M*)-diastereomers of assemblies $\mathbf{1x}_3$·((*R*)-MePheCYA)$_6$ as a result of the presence of chiral centers in the assembly[a]

1x	$\Delta G_{M/P}$ (kJ mol^{-1})[b]	ΔG_{tot} (kJ mol^{-1})[c]
1a	3.5	21.0
1b	4.2	25.2
1c	2.0	12.0

[a] [(*P*)-$\mathbf{1x}_3$•((R)-MePheCYA)$_6$] = [$\mathbf{1x}_3$•(BenCYA)$_6$] = 1.0 mM, 343 K, benzene. [b] Difference in free energy per chiral center. [c] Total free energy difference between (*P*)- and (*M*)-diastereomers of assemblies $\mathbf{1x}_3$·((*R*)-MePheCYA)$_6$.

assemblies. In this article we have shown that the amplification of chirality in these noncovalent assemblies can be modulated by the introduction of different substituents in the building blocks, that is calix[4]arene dimelamines or cyanurate derivatives. The introduction of sterically demanding substituents in the melamine moieties (R^1 substituents) decreases the amplification of chirality. Furthermore, the amplification of chirality is highly influenced by the presence of functional groups directly attached to the calix[4]arene skeleton (R^2 substituents). This influence might be due to the geometric constraints induced by these substituents in the assembly and/or electronic factors. On the contrary, the presence of bulky substituents in the cyanurate components leads to a large free energy difference (ΔG) between the diastereomers, and therefore to a large amplification of chirality. The introduction of nitro substituents in the calix[4]arene skeleton seems to influence the chiral amplification in the hydrogen-bonded assemblies the most, probably because of a decrease in the kinetics of the mixing process, leading to systems with a higher degree of chiral amplification. Therefore, future work will be aimed at the study of assemblies with a lower rate of dissociation of the dimelamine component of the assembly (a slow mixing process) and bulky cyanurates. The rate decrease could also be achieved by increasing the number of the hydrogen bonds that hold the components together. Possible candidates for this purpose are the tetrarosette assemblies in which the components

TABLE IV Differences in free energy calculated between the (*P*)- and (*M*)-diastereomers of assemblies $\mathbf{1a}_3$·(*CYA)$_6$ as a result of the presence of chiral centers in the assembly[a]

*CYA	$\Delta G_{M/P}$ (kJ mol^{-1})[b]	ΔG_{tot} (kJ mol^{-1})[c]
(*R*)-MePheCYA	3.5	21.0
(*L*)-PhealaCYA	2.3	13.8
(*L*)-ValCYA	2.3	13.8
(*R*)-MePropCYA	1.9	11.4
(*S*)-2-MeBuCYA	–	–

[a] [(*P*)-$\mathbf{1a}_3$·(*CYA)$_6$] = [$\mathbf{1a}_3$·(CYA)$_6$] = 1.0 mM, 343 K, benzene. [b] Difference in free energy per chiral center. [c] Total free energy difference between (*P*)- and (*M*)-diastereomers of assemblies $\mathbf{1a}_3$·(*CYA)$_6$.

TABLE III Differences in free energy calculated using the thermodynamic model between the (*P*)- and (*M*)-diastereomers of assemblies $\mathbf{1x}_3$·((*R*)-MePheCYA)$_6$[a]

1x	$\Delta G_{M/P}$ (kJ mol^{-1})[b]	ΔG_{tot} (kJ mol^{-1})[c]
1b	4.3	25.8
1e	4.2	25.2

[a] [(*P*)-$\mathbf{1x}_3$·((*R*)-MePheCYA)$_6$] = [$\mathbf{1x}_3$·(BenCYA)$_6$] = 1.0 mM, at 343 K, benzene. [b] Difference in free energy per chiral center. [c] Total free energy difference between (*P*)- and (*M*)-diastereomers of assemblies $\mathbf{1x}_3$·((*R*)-MePheCYA)$_6$.

are held together by the formation of 72 cooperative hydrogen bonds.

EXPERIMENTAL

THF was freshly distilled from Na/benzophenone, and CH_2Cl_2 from $CaCl_2$. All chemicals were of reagent grade and were used without further purification. NMR spectra were recorded on a Varian Unity 300 (^{1}H NMR 300 Hz) using tetramethylsilane (TMS) or the corresponding solvent as internal standard. FAB-MS spectra were recorded on a Finningan MAT 90 spectrometer with *m*-nitrobenzyl alcohol (NBA) as a matrix. CD spectra were recorded on a JASCO J-715 spectropolarimeter. Flash column chromatography was performed using silica gel (SiO_2, E. Merck, 0.040–0.063 mm, 230–400 mesh).

Assembly Formation

Assemblies were formed by dissolving the calix[4]-arene dimelamines **1** and the corresponding cyanurate (CYA/*CYA) in a 1:2 molar ratio in THF, after

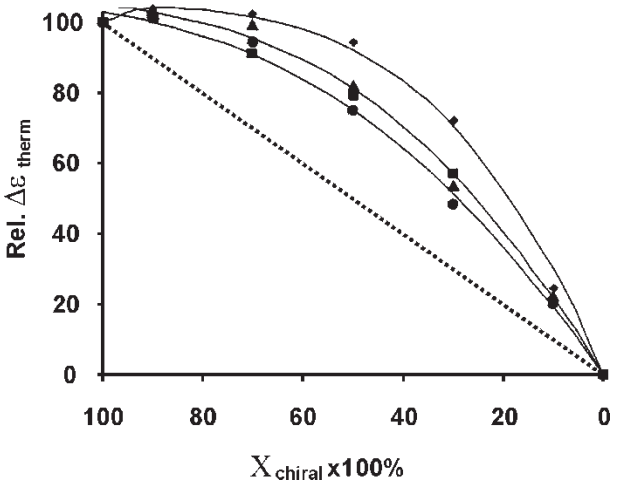

FIGURE 8 Plots of relative CD-intensities at thermodynamic equilibrium for different mole ratios of chiral component (*P*)-$\mathbf{1a}_3$·(*CYA)$_6$ for systems formed with (*P*)-$\mathbf{1a}_3$·(*CYA)$_6$ and $\mathbf{1a}_3$·(CYA)$_6$ (◆, (*R*)-MePheCYA/BenCYA; •, (*R*)-MePropCYA/BuCYA; ■, (*L*)-PhealaCYA/BenCYA; ▲, (*L*)-ValCYA/BuCYA). The solid lines represent the calculated best fit using the thermodynamic model described above. The dotted line represents the expected CD-intensity in the absence of amplification of chirality.

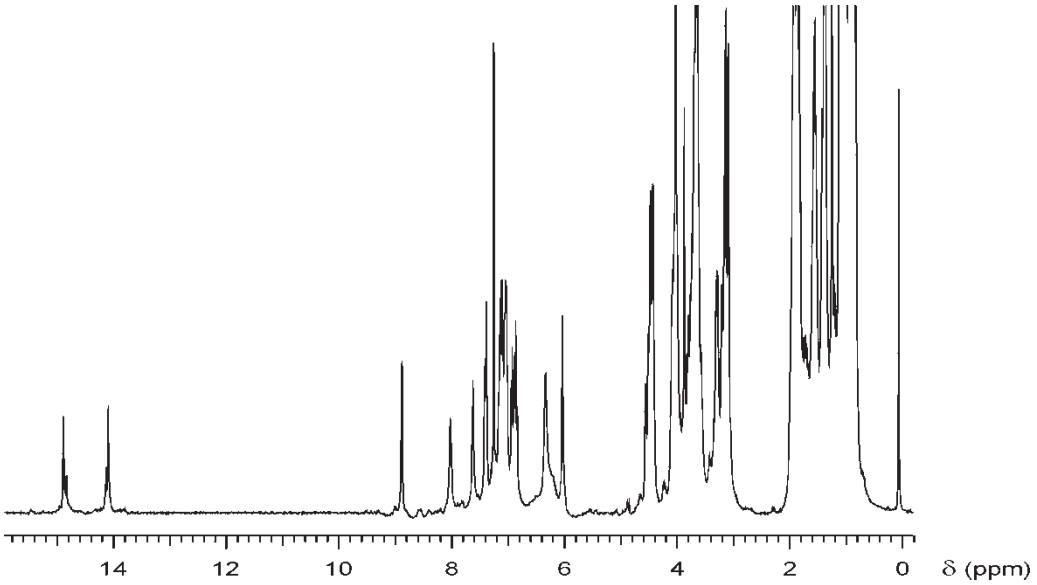

FIGURE 9 ^{1}H NMR spectrum of assembly $\mathbf{1a}_3$·((*S*)-2-MeBuCYA)$_6$. Spectra recorded in benzene-d_6 (300 MHz) at room temperature.

which the solvent was evaporated under high vacuum. After being dried under high vacuum, the assemblies were ready for use.

CD Titration Studies

Assembly solutions (1.0 mM) of the homomeric assemblies were mixed in ratios 90:10 to 10:90 at room temperature and injected into a thermostatted cell (0.01 cm width) immediately after mixing. The CD-intensities were monitored in time at constant temperature. The resulting plots were treated as described in the text.

Thermodynamic Model

The model was implemented in MicroMath Scientist for Windows, Version 2.01. The text file of the model is provided as supporting information.

Synthesis

The synthesis of compounds **1a**–**1c**, **1h**–**1j**, BuCYA, BenCYA, (*R*)-MePheCYA, (*L*)-PhealaCYA and (*L*)-ValCYA have been reported previously [33,35].

General Procedure for the Synthesis of Calix[4]arene Dimelamines 1d, 1f, 1g and 1e

A solution of bis(chlorotriazine) **1i**/**1j** (**1i** for **1d**, **1f** and **1g**, **1j** for **1e**), diisopropylethylamine (12 eq) and the corresponding amine (36 eq) in THF was refluxed for 1 week. The mixture was evaporated to dryness. The residue was dissolved in CH_2Cl_2, washed with water and brine, and the organic layer dried over Na_2SO_4. Evaporation of the organic solvent gave the corresponding calix[4]arene dimelamine **1** as a crude product, which was purified by column chromatography (SiO_2, CH_2Cl_2/MeOH/NH_4OH = 90/9.5/0.5%).

5,17-N,N′-Bis[4-amino-6-(2-methylethylamino)-1,3,5-triazin-2yl]diamino-25,26,27,28-tetrapropoxycalix[4]arene (1d)

Compound **1d** was prepared from calix[4]arene bis(chlorotriazine) **1i** (0.15 g, 0.16 mmol) and *i*-propylamine (0.5 mL) and was obtained as a white solid (74%). $R_f = 0.5$ (CH_2Cl_2/MeOH/NH_4OH 90:9:1); ^{1}H NMR (300 MHz, DMSO-d_6) δ 6.9–6.7 (br m, 6H, Ar*H*), 6.6–6.2 (br m, 4H, *o*-N*H*ArH + N*H*), 5.0–4.8 (br m, 6H, N*H*), 4.43, 3.10 (ABq, 8H, ^2J(H,H) = 13.5 Hz, ArCH_2-Ar), 4.01 (q, 2H, ^3J(H,H) = 6.6 Hz, NHC*H*$(CH_3)_2$), 3.93 (t, 4H, ^3J(H,H) = 6.6 Hz, OCH_2), 3.68 (t, 4H, ^3J(H,H) = 6.6 Hz, OCH_2), 2.0–1.8 (m, 8H, OCH$_2$CH_2), 1.15 (d, 12H, ^3J(H,H) = 6.6 Hz, NHCH(C$H_3)_2$), 1.03 (t, 6H, ^3J(H,H) = 7.5 Hz, O(CH$_2)_2$CH_3), 1.0–0.8 (t, 6H, ^3J(H,H) = 7.5 Hz, O(CH$_2)_2$CH_3). MS (FAB): m/z = 925.5 (100) ([M + H$^+$], calcd. 925.5). Anal. Calcd. for $C_{52}H_{68}N_{12}O_4$(%): C 67.51, N 18.17, H 7.41. Found: C 67.33, N 18.02, H 7.46.

5,17-N,N′-Bis[4-amino-6-(2-methylethylamino)-1,3,5-triazin-2yl]diamino-11,23-dinitro-25,26,27,28-tetrapropoxycalix[4]arene (1e)

Compound **1e** was prepared from calix[4]arene bis(chlorotriazine) **1j** (0.10 g, 0.10 mmol) and *i*-propylamine (0.3 mL) and was obtained as a white solid (65%). $R_f = 0.5$ (CH_2Cl_2/MeOH/NH_4OH 90:9:1); ^{1}H NMR (300 MHz, DMSO-d_6) δ 7.7(br s, 4H, *o*-NO2Ar*H*), 6.7–6.2 (m, 6H, *o*-NHArN*H* + N*H*), 5.0–4.9

(m, 6H, NH), 4.35, 3.18 (ABq, 8H, 2J(H,H) = 13.0 Hz, ArCH$_2$Ar), 3.98 (q, 2H, ^3J(H,H) = 6.6 Hz, NHCH(CH$_3$)$_2$), 3.95 (t, 4H, ^3J(H,H) = 6.6 Hz, OCH$_2$), 3.72 (t, 4H, ^3J(H,H) = 6.6 Hz, OCH$_2$), 2.0–1.8 (m, 8H, OCH$_2$CH$_2$), 1.15 (d, 12H, ^3J(H,H) = 6.6 Hz, NHCH(CH$_3$)$_2$), 1.03 (t, 6H, ^3J(H,H) = 7.5 Hz, O(CH$_2$)$_2$CH$_3$), 1.0–0.8 (t, 6H, ^3J(H,H) = 7.5 Hz, O(CH$_2$)$_2$CH$_3$). MS (FAB): m/z = 1015.3 (100) ([M + H$^+$], calcd. 1015.5). Anal. Calcd. for $C_{52}H_{66}N_{14}O_8$(%): C 61.52, N 19.32, H 6.55. Found: C 61.33, N 19.24, H 6.51.

5,17-N,N′-Bis[4-amino-6-(hexylamino)-1,3,5-triazin-2yl]diamino-25,26,27,28-tetrapropoxycalix[4]arene (1f)

Compound **1f** was prepared from calix[4]arene bis(chlorotriazine) **1i** (0.11 g, 0.12 mmol) and hexylamine (1.0 mL) and was obtained as a white solid (65%). R_f = 0.6 (CH$_2$Cl$_2$/MeOH/NH$_4$OH 90:9:1); ^{1}H NMR (300 MHz, DMSO-d_6) δ 7.0–6.7 (br m, 6H, ArH), 6.6–6.2 (br m, 4H, *o*-NHArH + NH), 5.0–4.8 (br m, 6H, NH), 4.43, 3.10 (ABq, 8H, ^2J(H,H) = 13.5 Hz, ArCH$_2$Ar), 3.93 (t, 4H, ^3J(H,H) = 6.6 Hz, OCH$_2$), 3.68 (t, 4H, ^3J(H,H) = 6.6 Hz, OCH$_2$), 3.31 (q, 4H, ^3J(H,H) = 6.3 Hz, NHCH$_2$) 2.0–1.8 (m, 8H, OCH$_2$CH$_2$), 1.9 (m, 8H, NHCH$_2$CH$_2$CH$_2$(CH$_2$)$_2$CH$_3$), 1.6–1.3 (m, 8H, NHCH$_2$CH$_2$CH$_2$(CH$_2$)$_2$CH$_3$) 1.15 (t, 6H, ^3J(H,H) = 7.4 Hz, O(CH$_2$)$_2$CH$_3$), 1.0–0.8 (m, 12H, NH(CH$_2$)$_5$CH$_3$ + O(CH$_2$)$_2$CH$_3$). MS (FAB): m/z = 1009.7 (100) ([M + H$^+$], calcd. 1009.2). Anal. Calcd. for $C_{58}H_{80}N_{12}O_4$(%): C 68.89, N 16.58, H 8.01. Found: C 68.53, N 16.42, H 8.46.

5,17-N,N′-Bis[4-amino-6-(2,2-dimethylethylamino)-1,3,5-triazin-2yl]diamino-25,26,27,28-tetrapropoxycalix[4]arene (1g)

Compound **1g** was prepared from calix[4]arene bis(chlorotriazine) **1i** (0.15 g, 0.16 mmol) and *t*-butylamine (0.6 mL) and was obtained as a white solid (76%). R_f = 0.6 (CH$_2$Cl$_2$/MeOH/NH$_4$OH 90:9:1); ^{1}H NMR (300 MHz, DMSO-d_6) δ 7.4–7.1 (br m, 6H, ArH), 6.6–6.2 (br m, 4H, *o*-NHArH + NH), 5.0–4.8 (br m, 6H, NH), 4.35, 3. 05 (ABq, 8H, ^2J(H,H) = 13.5 Hz, ArCH$_2$-Ar), 3.86 (t, 4H, ^3J(H,H) = 6.6 Hz, OCH$_2$), 3.62 (t, 4H, ^3J(H,H) = 6.6 Hz, OCH$_2$), 2.0–1.8 (m, 8H, OCH$_2$CH$_2$), 1.58 (s, 18H, NC(CH$_3$)$_3$), 1.15 (t, 6H, ^3J(H,H) = 7.4 Hz, O(CH$_2$)$_2$CH$_3$), 1.0–0.8 (m, 6H, O(CH$_2$)$_2$CH$_3$). MS (FAB): m/z = 953.6 (100) ([M + H$^+$], calcd. 953.5). Anal. Calcd. for $C_{54}H_{72}N_{12}O_4$(%): C 68.04, N 17.63, H 7.61. Found: C 67.89, N 17.88, H 7.69.

General Procedure for the Synthesis of the Cyanurates (*R*)-MePropCYA and (*S*)-2-MeBuCYA [39]

The reaction was performed under flame-dried conditions and a continuous flow of argon. The argon was led through water to trap phosgene formed before leaving the reaction system. The corresponding amine was suspended in THF and *N*-chlorocarbonylisocyanate (2 eq) was added slowly. After stirring at room temperature for 2 h, the reaction mixture was refluxed for 2 days. After evaporation of the solvent, the residue was redissolved in CH$_2$Cl$_2$, washed with water, dried over Na$_2$SO$_4$ and purified by column chromatography (SiO$_2$, CH$_2$Cl$_2$/-MeOH/NH$_4$OH: 90/9.5/0.5).

N-((R)-1-methylpropyl)-1,3,5-triazine-2,4,6(1H,3H,5H)-trione (= (R)-MePropCYA)

Compound (*R*)-MePropCYA was prepared from (*R*)-sec-butylamine (0.5 mL, 5 mmol) and *N*-chlorocarbonylisocyanate (0.8 mL, 10 mmol) and was obtained as a white solid (34%). R_f = 0.4 (CH$_2$Cl$_2$/MeOH/NH$_4$OH 90:9:1); ^{1}H NMR (300 MHz, DMSO-d_6) δ 11.32 (s, 2H, NH), 4.44–4.58 (m, 1H, N*CH), 1.82-1.99 (m, 1H, CH$_2$CH$_3$), 1.57-1.73 (m, 1H, CH$_2$CH$_3$), 1.31 (d, 3H, 3J(H,H) = 7.0 Hz, *CHCH$_3$), 0.79 (m, 3H, CH$_2$CH$_3$). MS (FAB): m/z = 184.0 (100) ([M − H$^+$], calcd. 184.1). Anal. Calcd. for $C_7H_{11}N_3O_3$(%): C 45.40, N 22.69, H 5.99. Found: C 45.66, N 22.49, H 5.78.

N-((S)-2-methylbutyl)-1,3,5-triazine-2,4,6(1H,3H,5H)-trione (= (S)-2-MeBuCYA)

Compound (*S*)-2-MeBuCYA was prepared from (*S*)-2-methylbutylamine (0.6 mL, 5 mmol) and *N*-chlorocarbonylisocyanate (0.8 mL, 10 mmol) and was obtained as a white solid (20%). R_f = 0.4 (CH$_2$Cl$_2$/MeOH/NH$_4$OH 90:9:1); ^{1}H NMR (300 MHz, DMSO-d_6) δ 11.38 (s, 2H, NH), 3.53 (m, 2H, ^3J(H,H) = 5.4 Hz, NCH$_2$), 1.74 (d, 2H, ^3J(H,H) = 5.4 Hz, CHCH$_3$), 1.32 (m, 1H, NCH$_2$CHCH$_3$CHH), 1.08 (m, 1H, NCH$_2$ CHCH$_3$CH H), 0.80 (m, 3H, CH$_2$CH$_3$). ^{13}C NMR (75 MHz, DMSO-d_6), δ 150.1, 45.8, 32.6, 26.3, 16.4, 10.9. MS (FAB): m/z = 200.1 (100) ([M + H$^+$], calcd. 200.1). Anal. Calcd. for $C_8H_{13}N_3O_3$(%): C 48.23, N 21.09, H 6.58. Found: C 48.29, N 21.00, H 6.65.

References

[1] Feringa, B. L.; van Delden, R. A. *Angew. Chem. Int. Ed. Engl.* **1999**, *38*, 3418.
[2] Shibata, T.; Yamamoto, J.; Matsumoto, N.; Yonekubo, S.; Onsanai, S.; Soai, K. *J. Am. Chem. Soc.* **1998**, *120*, 12157.
[3] Sato, T.; Urabe, H.; Ishiguro, S.; Shibata, T.; Soai, K. *Angew. Chem., Int. Ed. Engl.* **2003**, *42*, 315.
[4] Kitamura, M.; Suga, S.; Oka, H.; Noyori, R. *J. Am. Chem., Soc.* **1998**, *120*, 9800.
[5] Girard, C.; Kagan, H. *Angew. Chem. Int. Ed. Engl.* **1998**, *37*, 2992.
[6] Green, M. M.; Rediy, M. P.; Johnson, R. J.; Darling, G.; O'Leary, D. J.; Wilson, G. J. *J. Am. Chem. Soc.* **1989**, *111*, 6452.
[7] Green, M. M.; Peterson, N. C.; Sato, T.; Teramoto, A.; Cook, R.; Lifson, S. *Science* **1995**, *268*, 1860.

[8] Green, M. M.; Park, J.-W.; Sato, T.; Teramoto, A.; Lifson, S.; Selinger, R. L.; Selinger, J. W. *Angew. Chem. Int. Ed. Engl.* **1999**, *38*, 3138.
[9] Green, M. M.; Cheon, K.-S.; Yang, S.-Y.; Park, J.-W.; Swansburg, S.; Liu, W. *Acc. Chem. Res.* **2001**, *34*, 672.
[10] Palmans, A. R. A.; Vekemans, J. A. J. M.; Havinga, E. E.; Meijer, E. W. *Angew. Chem., Int. Ed. Engl.* **1997**, *36*, 2648.
[11] Brunsveld, L.; Schenning, A. P. H. J.; Broeren, M. A. C.; Janssen, H. M.; Vekemans, J. A. J. M.; Meijer, E. W. *Chem. Lett.* **2000**, 292.
[12] Brunsveld, L.; Lohmeijer, B. G. G.; Vekemans, J. A. J. M.; Meijer, E. W. *Chem. Commun.* **2000**, 2305.
[13] Schenning, A. P. H. J.; Jonkheijm, P.; Peeters, E.; Meijer, E. W. *J. Am. Chem. Soc.* **2001**, *123*, 409.
[14] Brunsveld, L.; Meijer, E. W.; Prince, R. B.; Moore, J. S. *J. Am. Chem. Soc.* **2001**, *123*, 7978.
[15] Masuda, M.; Honkheijm, P.; Sijbesma, R. P.; Meijer, E. W. *J. Am. Chem. Soc.* **2003**, *125*, 15935.
[16] Van Gestel, J.; Van der Schoot, P.; Michels, M. A. J. *Macromolecules* **2003**, *36*, 6668.
[17] Teramoto, A. *Prog. Polym. Sci.* **2001**, *26*, 667.
[18] Selinger, J. V.; Selinger, R. L. B. *Phys. Rev. E* **1997**, *55*, 1728.
[19] Gu, H.; Sato, T.; Teramoto, A.; Varichon, L.; Green, M. M. *Polym. J.* **1997**, *29*, 77.
[20] Lifson, S.; Andreola, C.; Peterson, N. C.; Green, M. M. *J. Am. Chem. Soc.* **1989**, *111*, 8850.
[21] Saxena, A.; Guo, G.; Fujiki, M.; Yang, Y.; Ohira, A.; Okoshi, K.; Naito, M. *Macromolecules* **2004**, *37*, 3081.
[22] Yashima, E.; Matsushima, T.; Okamoto, Y. *J. Am. Chem. Soc.* **1997**, *119*, 6345.
[23] Yashima, E.; Maeda, K.; Nishimura, T. *Chem. Eur. J.* **2004**, *10*, 42.
[24] Ishi-i, T.; Crego-Calama, M.; Timmerman, P.; Reinhoudt, D. N.; Shinkai, S. *J. Am. Chem. Soc.* **2002**, *124*, 14631.
[25] Fenniri, H.; Deng, B.-L.; Ribbe, A. E. *J. Am. Chem. Soc.* **2002**, *124*, 11064.
[26] Mizuno, Y.; Aida, T. *Chem. Commun.* **2003**, 20.
[27] Oda, M.; Nothofer, H.-G.; Lieser, G.; Schref, U.; Meskers, S. C. J.; Neher, D. *Adv. Mater.* **2000**, *12*, 362.
[28] Link, D. R.; Natale, G.; Saho, R.; Maclennan, J. E.; Clark, N. A.; Körblova, E.; Walba, D. M. *Science* **1997**, *278*, 1924.
[29] Trzaska, S. T.; Hsu, H.-F.; Swager, T. M. *J. Am. Chem. Soc.* **1999**, *121*, 4518.
[30] Barberá, J.; Cavero, E.; Lehmann, M.; Serrano, J.-L.; Sierra, T.; Vázquez, J. T. *J. Am. Chem. Soc.* **2003**, *125*, 4527.
[31] Prins, L. J.; Timmerman, P.; Reinhoudt, D. N. *J. Am. Chem. Soc.* **2001**, *123*, 10153.
[32] Vreekamp, R. H.; Van Duynhoven, J. P. M.; Hubert, M.; Verboom, W.; Reinhoudt, D. N. *Angew. Chem. Int. Ed. Engl.* **1996**, *35*, 1215.
[33] Timmerman, P.; Vreekamp, R. H.; Hulst, R.; Verboom, W.; Reinhoudt, D. N.; Rissanen, K.; Udachin, K. A.; Ripmeester, J. *Chem. Eur. J.* **1997**, *3*, 1823.
[34] Prins, L. J.; Jolliffe, K. A.; Hulst, R.; Timmerman, P.; Reinhoudt, D. N. *J. Am. Chem. Soc.* **2000**, *122*, 3617.
[35] Prins, L. J.; Huskens, J.; De Jong, F.; Timmerman, P.; Reinhoudt, D. N. *Nature* **1999**, *398*, 498.
[36] Prins, L. J.; Hulst, R.; Timmerman, P.; Reinhoudt, D. N. *Chem. Eur. J.* **2002**, *8*, 2288.
[37] Prins, L. J.; De Jong, F.; Timmerman, P.; Reinhoudt, D. N. *Nature* **2000**, *408*, 181.
[38] Prins, L. J.; Verhage, J. J.; De Jong, F.; Timmerman, P.; Reinhoudt, D. N. *Chem. Eur. J.* **2002**, *8*, 2302.
[39] Kimizuka, N.; Kawasaki, T.; Hirata, K.; Kunitake, T. *J. Am. Chem. Soc.* **1998**, *120*, 4094.

SUPPORTING INFORMATION

Controlling the Amplification of Chirality in Noncovalent Assemblies

Molecular Mechanics Calculations

Initial structures, created by manual modification of the X-ray structure of a double- rosette assembly [1s], and by observed NOE connectivities used as distance constraints, as well as visualizations, were carried out with Quanta 97 [2s]. The MD calculations were run with CHARMm, version 24.0 [3s]. Parameters were taken from Quanta 97, and point charges were assigned with the charge template option in Quanta/CHARMm; excess charge was smoothened, rendering overall neutral residues. A distance-dependent dielectric constant was applied with $\varepsilon = 1$. No cutoffs on the nonbonded interactions were used. Energy minimizations were performed with the Steepest Descent and Adopted Basis Newton–Raphson methods until the root mean square of the energy gradient was $< 0.001\,\mathrm{kcal\,mol^{-1}\,\AA^{-1}}$.

[1s] Timmerman, P.; Vreekamp, R. H.; Hulst, R.; Verboom, W.; Reinhoudt, D. N.; Rissanen, K.; Udachin, K. A.; Ripmeester, J. *Chem. Eur. J.* **1997**, *3*, 1823.
[2s] Quanta97, *Molecular Simulations*, Waltham, MA (1997).
[3s] (a) Brooks, B. R.; Bruccoleri, R. E.; Olafsen, B. D.; States, D. J.; Swaminathan, S.; Karplus, M. *J. Comput. Chem.* **1983**, *4*, 187; (b) Momany, F. A.; Klimkowski, V. J.; Schäfer, L. *J. Comput. Chem.* **1990**, *11*, 654; (c) Momany, F. A.; Rone, R.; Kunz, H.; Frey, R. F.; Newton, S. Q.; Schäfer, L. *J. Mol. Struct*. **1993**, *286*, 1.

Thermodynamic Model

This model is implemented in MicroMath® Scientis® for Windows, Version 2.01.

```
// MicroMath Scientist Model File

IndVars: RTOT

DepVars: S, R, B, PR6, MR6, PR5B1, MR5B1, PR4B2, MR4B2, PR3B3, MR3B3,

PR2B4, MR2B4, PR1B5, MR1B5, PB6, MB6

Params: SF, KROS, fm

PR6=KROS*R^6

MR6=fm^6*KROS*R^6

PR5B1−6*KROS*R^5*B

MR5B1=6*fm^5*KROS*R^5*B

PR4B2  15*KROS*R^4*B^2

MR4B2=15*fm^4*KROS*R^4*B^2

PR3B3−20*KROS*R^3*B^3

MR3B3=20*fm^3*KROS*R^3*B^3

PR2B4=15*KROS*R^2*B^4

MR2B4=15*fm^2*KROS*R^2*B^4

PR1B5=6*KROS*R*B^5

MR1B5−6*fm*KROS*R*B^5

PB6=KROS*B^6

MB6  KROS*B^6

RROS=6*PR6+5*PR5B1+4*PR4B2−3*PR3B3+2*PR2B4+PR1B5−6*MR6+5*MR5B

1+4*MR4B2+3*MR3B3+2*MR2B4+MR1B5

R=RTOT-RROS

BROS=6*PB6+5*PR1B5+4*PR2B4+3*PR3B3+2*PR4B2+PR5B1−6*MB6+5*MR1B

5+4*MR2B4+3*MR3B3+2*MR4B2+MR5B1

B−6-RTOT-BROS

P−PR6+PR5B1+PR4B2+PR3B3+PR2B4+PR1B5+PB6

M=MR6+MR5B1−MR4B2+MR3B3+MR2B4+MR1B5+MB6

S=SF*((P-M)/(P+M))

0.0<R<1

0.0<B<1

***
```

with RTOT = total concentration of chiral cyanurate *CYA; S = CD-intensity; R = concentration of *CYA; B = concentration of CYA; SF = scaling factor; $f_m = \exp(-\Delta G^\circ_{P/M}/RT)$; KROS = 10^{10}. In this model the composition of the assemblies is given by the letters R and B (R for *CYA and B for CYA) and the chirality of the assembly by the letter M or P.